Articles

Resilience of *Rhodobacter sphaeroides* Cytochrome bc_1 to Heme c_1 Ligation Changes†

Haibo Zhang,‡ Artur Osyczka,§ Christopher C. Moser,‡ and P. Leslie Dutton*,‡

The Johnson Research Foundation, Department of Biochemistry and Biophysics, University of Pennsylvania, Philadelphia, Pennsylvania 19104, and Faculty of Biochemistry, Biophysics and Biotechnology, Jagiellonian University, Kraków, Poland

Received July 3, 2006; Revised Manuscript Received September 18, 2006

ABSTRACT: Typically, *c* hemes are bound to the protein through two thioether bonds to cysteines and two axial ligands to the heme iron. In high-potential class I *c*-type cytochromes, these axial ligands are commonly His-Met. A change in this methionine axial ligand is often correlated with a dramatic drop in the heme redox potential and loss of function. Here we describe a bacterial cytochrome *c* with an unusual tolerance to the alternations in the heme ligation pattern. Substitution of the heme ligating methionine (M185) in cytochrome c_1 of the *Rhodobacter sphaeroides* cytochrome bc_1 complex with Lys and Leu lowers the redox midpoint potential but not enough to prevent physiologically competent electron transfer in these fully functional variants. Only when Met-185 is replaced with His is the drop in the redox potential sufficiently large to cause cytochrome bc_1 electron transfer chain failure. Functional mutants preserve the structural integrity of the heme crevice: only the nonfunctional His variant allows carbon monoxide to bind to reduced heme, indicating a significant opening of the heme environment. This range of cytochrome c_1 ligand mutants exposes both the relative resilience to sixth axial ligand change and the ultimate thermodynamic limits of operation of the cofactor chains in cytochrome bc_1.

c-Type cytochromes play a central role in biological electron transfer systems and have been a popular subject in the probing of the engineering of biological redox reactions. Unlike *b* hemes which are linked to protein by only one or two axial ligands to the heme iron, *c* hemes are commonly bound by an additional pair of thioether bonds to cysteines. A His-Met ligation to heme iron provides the common signature for a high-potential class I *c*-type cytochrome (*1*−*5*).

As one of the subunits of the catalytic core of the cytochrome bc_1 complex, cytochrome c_1 structurally links the core subunits and provides a pair of surface docking sites for its two usual redox partners, the mobile iron−sulfur subunit and cytochrome *c* (cytochrome c_2 in bacteria). Its extrinsic domain shares many of the electrochemical and structural properties of class I *c*-type cytochromes with some distinguishing structure−function related insertions or deletions in the loop region (*6*−*9*). Cytochrome c_1 of some bacterial species has a unique disulfide bond anchoring loop, which is not present in the sequences of cytochrome c_1 of higher organisms (*6*−*10*; Figure 1).

The mature cytochrome c_1 from *Rhodobacter sphaeroides* has 263 amino acids after a 22-residue amino-terminal signal sequence is removed from the precursor (*11*, *12*; see Figure 1c for the primary structure). The consensus heme-binding motif (CXXCH) located near the N-terminus provides the cysteines for the covalent attachment of the heme group and the invariant histidine as the fifth axial ligand. With respect to the opposite, carboxyl terminus, the hydropathy profile of the sequence of the mature polypeptide identifies a single transmembrane α-helix (from A229 to K249) that can anchor the subunit to the membrane (*11*). Truncation of this anchor yields a soluble form of cytochrome c_1 (*13*). A comparison of the sequences of cytochrome c_1 from *Rb. sphaeroides* and *Rb. capsulatus* reveals a very close evolutionary kinship (*14*).

As for any other redox protein, the redox midpoint potential (E_m)[1] is a key property of cytochrome c_1 that regulates biological functions via thermodynamic and kinetic control of electron-exchange reactions. Extensive work has been devoted to unraveling the complex interplay of molecular factors that modulate E_m, including several studies aimed at the effect of sixth axial ligand methionine on the function of cytochrome *c* and c_1 in eukaryotic and prokaryotic

† This work has been support by NIH Grant GM27309 to P.L.D.

* To whom correspondence should be addressed: 1005 Stellar-Chance labs, 422 Curie Blvd., Department of Biochemistry and Biophysics, University of Pennsylvania, Philadelphia, PA 19104-6059. Phone: (215) 898-0991. Fax: (215) 573-2235. E-mail: dutton@mail.med.upenn.edu.

‡ University of Pennsylvania.

§ Jagiellonian University.

[1] Abbreviations: FeS, two-iron−two-sulfur cluster; SDS−PAGE, sodium dodecyl sulfate−polyacrylamide gel electrophoresis; Q, ubiquinone; QH_2, ubihydroquinone; E_m, redox midpoint potential; E_h, ambient redox potential; SHE, standard hydrogen electrode; TMBZ, tetramethylbenzidine; βXM, three-amino acid motif starting with a β-branched amino acid and ending in methionine; Ps+ and Ps−, photosynthetic competence and incompetence, respectively.

10.1021/bi061345i CCC: $33.50
Published on Web 11/09/2006

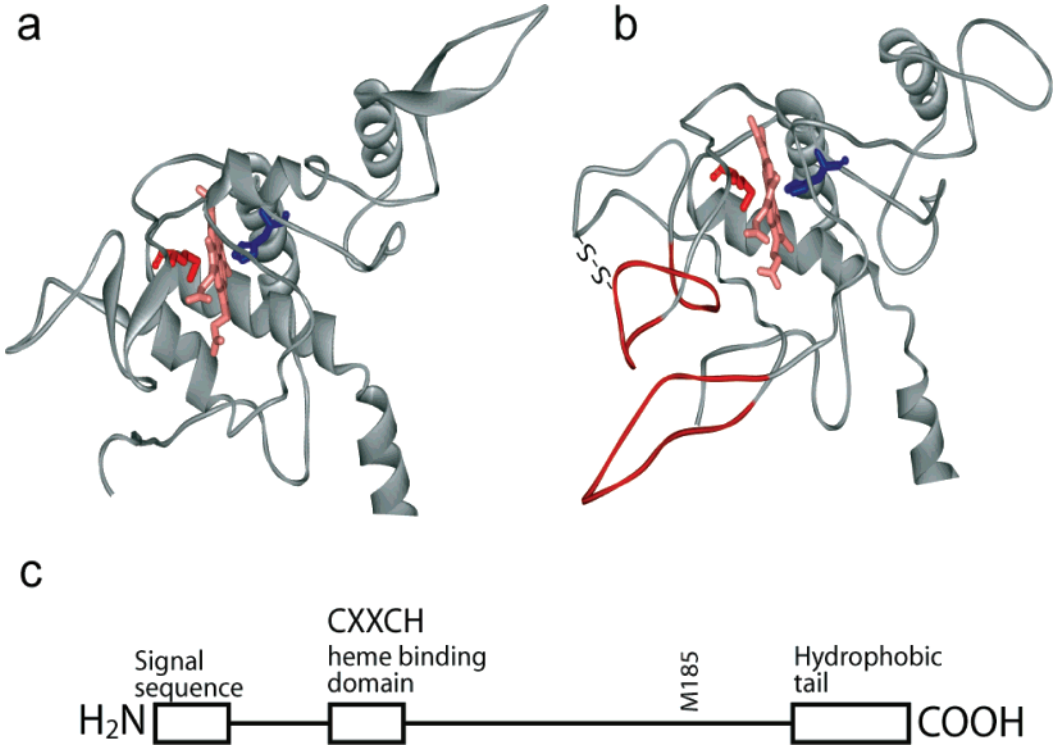

FIGURE 1: Comparison of the redox active head regions of mitochondrial yeast (*42*) (a) and bacterial cytochrome c_1 (*6*) (b). The heme (pink) is axially ligated by histidine (blue) and methionine (red). The red ribbons highlighted in bacterial cytochrome c_1 are the two major inserts, including a disulfide-anchored loop. Panel c shows the schematic diagram of the primary organization of the cytochrome c_1 polypeptide.

species (see examples in refs *5* and *15*−*23*). All these studies indicated that the nature of the sixth axial ligand plays a critical role in controlling the biological function and structure in cytochrome *c* and c_1 by altering the refolding pattern in addition to the redox midpoint potential.

Here we describe a bacterial cytochrome *c* with an unusual tolerance to the change in the heme ligation pattern. We constructed three variants: two which could in principle replace methionine as a sixth ligand, namely, lysine (K) and histidine (H), and one, namely, leucine (L), that should not be able provide ligation to the heme iron. We revealed a very unusual example of *c*-type heme protein in which the sixth ligand can be mutated without a destructive impact on its E_m. Mutating the heme-ligating methionine (M185) to Lys and Leu yields fully functional variants of the enzymes that, despite significant changes in spectra and redox properties, keep the potential of the heme sufficiently high to support physiologically competent electron transfer. The histidine mutant drags the potential low enough to render the cytochrome functionally incompetent. Functional mutants maintain the structural integrity of the heme crevice, while the dysfunctional histidine does not. Met-185 mutants in *Rb. sphaeroides* reveal a certain resilience of the sixth axial ligand domain in this cytochrome *c* and define the limits of this resilience when a redox potential falls too far out of line with others in a redox chain.

MATERIALS AND METHODS

Bacterial Strains and Growth. *Escherichia coli* and *Rb. sphaeroides* strains were grown in the presence of appropriate antibiotics as described previously (*11*). Respiratory growth of *Rb. sphaeroides* strains occurred at 32 °C in the dark under semiaerobic conditions, and photosynthetic growth (Ps) occurred at the same temperature under continuous light and anaerobic conditions. BC17 is a cytochrome bc_1 strain where the chromosomal copy of the *fbc* operon has been deleted (*11*). Strain BC17C corresponds to BC17 complemented in trans with the plasmid pRK415-*fbc*, which contains a wild-type copy of the *fbc* operon and a tetracycline resistance cartridge. This strain is considered the wild-type reference in this study. Mutant strains M185L/BC17, M185K/BC17, and M185H/BC17 are identical to BC17C, except that the codon corresponding to M185 of the *fbc* operon has been mutated to encode leucine, lysine, and histidine, respectively.

Molecular Genetic Techniques. The mutations were constructed by site-directed mutagenesis using the Quikchange system from Stratagene and the pbc9 plasmid [a derivative of pUC9 containing a wild-type copy of the *fbc* operon (*11*)] as template DNA. The following mutagenic primers were used to introduce single mutations (F and R denote forward and reverse, respectively): 5′-CTC GTG GAT CGC C**TT G**CC GCC TCC GCT C-3′ (M185L-F), 5′-GAG CGG AGG CGG **CAA** GGC GAT CCA CGA G-3′ (M185L-R), 5′-CTC GTG GAT CGC C**CA C**CC GCC TCC GCT C-3′ (M185H-F), 5′-GAG CGG AGG CGG **GTG** GGC GAT CCA CGA G-3′ (M185H-R), 5′-CTC GTG GAT CGC C**AA A**CC GCC TCC GCT C-3′ (M185K-F), and 5′-GAG CGG AGG CGG **TTT** GGC GAT CCA CGA G-3′ (M185K-R). After sequencing had been carried out, the appropriate DNA fragments bearing the desired mutation and no other mutations were inserted into pRK415 [the expression vector containing a tetracycline resistance cartridge (*11*, *24*)] using the restriction enzymes *Hin*dIII and *Eco*RI. The mutated variants of pRK415-*fbc* were introduced into strain BC17 via triparental crosses. The presence of engineered mutations was confirmed by sequencing the plasmid DNA isolated from mutated *Rb. sphaeroides* strains.

Table 1: Various Properties of *Rb. sphaeroides* Cytochrome c_1 Sixth Axial Ligand Species

strain	phenotype[a]	E_{m7} (mV)[b]	b_H reduction rate (s^{-1})[c]	CO binding[d]	reversion to Ps+[e]
wild type	PS+	268	856	−	
M185L	PS+	216	85	−	
M185K	PS+	130	20	−	
M185H	PS−	74	0[f]	+	M185Y, M185L
M185Y	PS+	241, 132	62	−	

[a] Ps+ and Ps− denote photosynthetic competence and incompetence, respectively. [b] Midpoint redox potential of cytochrome c_1 in chromatophore membranes. [c] b_H reduction rates were determined by flash kinetics at the ambient potential of 100 mV at pH 7.0 by recording the absorbance changes at 560−570 nm and fitting them to a single-exponential equation. [d] + and − indicate the ability of ferrocytochrome c_1 in isolated cytochrome bc_1 to bind carbon monoxide in a gas-saturated solution. [e] Spontaneous site suppressor mutations in cytochrome c_1 that restore the photosynthetic activity of the cells. [f] At the standard redox poise of 100 mV, more than half of this mutant cytochrome c_1 will be oxidized even before flash oxidation of cytochrome c_2. In principle, the rate with fully reduced c_1 could be even slower.

Spontaneous Ps+ revertants of the M185H mutant were obtained on Sistrom's A plates containing tetracycline over several days of incubation under selective photosynthetic conditions. The plasmids of the PS+ revertants were extracted and sequenced to determine the location and nature of the suppressor mutations. The entire *fbc*C gene was subjected to DNA sequence analysis. The fragment of *fbc*C containing the reversion (H185Y) was exchanged with its counterpart on pbc9. The plasmid that was obtained was conjugated into pRK415 and crossed with *Rb. sphaeroides* strain BC17 to produce the M185Y mutant that expressed the cytochrome bc_1 complex containing the reversion used to further biochemical analysis.

Biochemical and Biophysical Techniques. Chromatophore membranes and purified cytochrome bc_1 were prepared as described previously (*25*, *26*) with a DEAE-Sepharose column (Amersham Pharmacia). Sodium dodecyl sulfate−polyacrylamide gel electrophoresis (SDS−PAGE) was performed according to the method of Laemmli (*27*) using a 15% linear separating gel. The gels were stained with Coomassie blue for proteins or with tetramethylbenzidine (TMBZ) for covalently attached hemes (*28*).

Optical spectra were recorded on a Perkin-Elmer UV−vis spectrophotometer (Lambda 20) fitted with an anaerobic redox cuvette when necessary. The difference spectra for *c*- and *b*-type cytochrome were obtained with samples that were first oxidized by an addition of potassium ferricyanide and then reduced by using either sodium ascorbate or fresh sodium dithionite.

Dark equilibrium redox titrations of the heme groups were performed as described previously (*29*). Chromatophore membranes or the purified cytochrome bc_1 was suspended in MOPS buffer (pH 7.0) containing 100 mM KCl and redox mediators: 2,3,5,6-tetramethylphenylenediamine, 1,2-naphthoquinone 4-sulfonate, 1,2-naphthoquinone, phenazine, methosulfate, phenazine ethosulfate, duroquinone, pyocyanine, indigo trisulfonate, 2-hydroxy-1,4-naphthoquinone, phenazine, anthraquinone 2-sulfonate, and benzyl viologen. The optical changes that accompanied redox potential change were recorded in the α-band region (500−600 nm) or in the Soret region (400−450 nm), and the E_m values were determined by fitting the data to an $n = 1$ Nerst equation, with one, two, or three components, as necessary.

Flash-induced single-turnover time-resolved kinetics were determined according to the method described in ref *30* using chromatophore membranes and a double-beam spectrophotometer (Biomedical Instrumentation Group, University of Pennsylvania) in the presence of 2.5 μM valinomycin, 8 μM 2,3,5,6-tetramethylphenylenediamine, 2.5 μM phenazine methosulfate, 2.5 μM phenazine ethosulfate, 6 μM 1,2-naphthoquinone, 6 μM 2-hydroxy-1,4-naphthoquinone, 100 μM ferrocyanide, and 70 μM benzyl viologen. Transient cytochrome b_H reduction kinetics followed at 560−570 nm were initiated by a short saturating flash (8 μs) from a xenon lamp. The concentrations of antimycin, myxothiazol, and stigmatellin that were used were 5, 5, and 1 μM, respectively, and the ambient potential was poised at 100 mV.

The carbon monoxide (CO) binding experiments were performed at room temperature using a sealed anaerobic cuvette. Purified, intact cytochrome bc_1 dissolved in 50 mM Tris-HCl (pH 8.0) containing 100 mM KCl was deoxygenated with argon and then reduced by an anaerobic addition of sodium dithionite. The CO was then introduced into the samples by brief bubbling to produce the dithionite-reduced + CO versus dithionite-reduced spectra.

RESULTS

We constructed three single mutants of the sixth axial ligand of heme c_1 in cytochrome bc_1 of *Rb. sphaeroides* and expected severe structural and/or functional consequences. Similar mutations in yeast (*22*) had destructive effects on assembly, while in closely related *Rb. capsulatus*, cytochrome bc_1 photosynthetic electron transfer function was lost (*16*, *20*). Surprisingly, two mutants, M185L and M185K, are capable of photosynthetic growth (Table 1), indicating that cytochrome bc_1 is functional in vivo. Only M185H was unable to support the photosynthetic growth. We employed a series of biochemical and spectroscopic examinations to understand the roots of these unexpected phenotypes and identify physical and chemical changes that turn functional mutants into nonfunctional mutants.

Assembly of M185 Mutants. Subunit composition analysis using SDS−PAGE and TMBZ heme staining of the cytochrome bc_1 isolated from the mutated strains revealed that the expressed bc_1 complexes in all mutants contain four subunits and the heme group covalently attached to cytochrome c_1, no different from the native protein (Figure 2). This excludes the assembly factor as a primary cause of phenotypic differences seen between the functional (M185L and M185K) and nonfunctional (M185H) mutants.

Spectroscopic Properties of M185 Mutants. The optical difference spectra of chromatophores and purified cytochrome bc_1 showed that all M185 mutants induce significant changes in the spectral properties of heme c_1. While

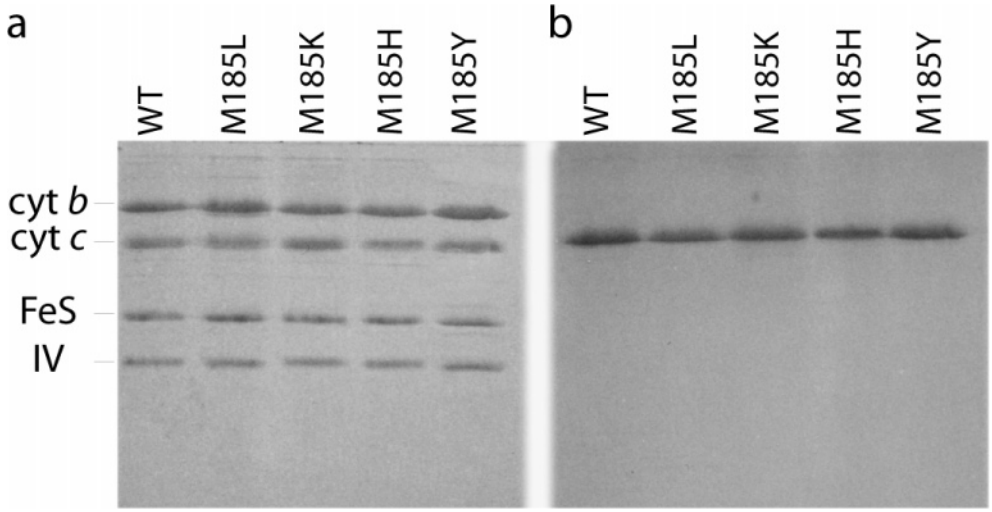

FIGURE 2: SDS−PAGE analysis of cytochrome bc_1 isolated from the wild type and cytochrome c_1 methionine mutants: M185L, M185K, M185H, and M185Y. The gels were stained for proteins with Coomassie blue (a) and for heme *c* with TMBZ (b).

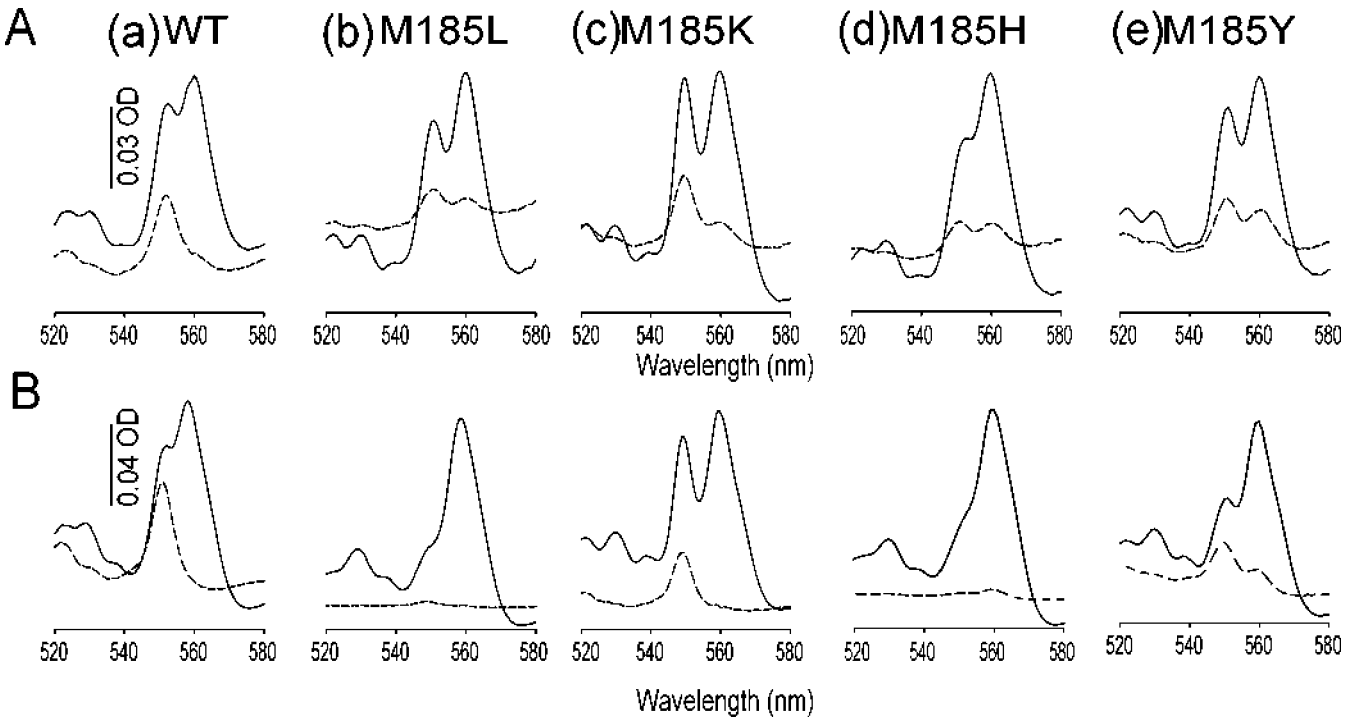

FIGURE 3: Optical difference spectra of various chromatophore membranes (A) and purified cytochrome bc_1 (B). Spectra were recorded using samples at the same concentration in 50 mM MOPS (pH 7.0) and 100 mM KCl with a 1 cm optical path length. Solid and dashed lines correspond to dithionite minus ferricyanide and ascorbate minus ferricyanide spectra, respectively.

chromatophore redox difference spectra (Figure 3A) are complicated by unavoidable contributions from other *c*-type cytochromes, these contributions are eliminated in the simple spectra of purified cytochrome bc_1 (Figure 3B). The wild-type spectra are characterized by the presence of both ascorbate and dithionite-reducible components (Figure 3Aa,-3Ba). In the α-region, the ascorbate-reducible component at 552 nm (dashed line) reflects the reduced state of heme c_1, while the dithionite-reducible (solid line) components include heme c_1 and hemes b_L and b_H (peak at 560 nm). The only mutant which has a clear ascorbate-reducible component in both chromatophores (Figure 3Ac, dashed line) and purified complexes (Figure 3Bc) is M185K. This mutant exhibits a clear red shift to 550 nm, similar to the analogous M183K ligand mutant of *Rb. capsulatus* (*16*). On the other hand, both M185L and M185H mutants show minimal ascorbate-reducible components in chromatophores (Figure 3Ab,d, dashed line) and none in the purified cytochrome (Figure 3Bb,d, dashed line). Further reduction of chromatophores and purified cytochrome from M185L and M185H by dithionite reveals a conspicuous 560 nm peak corresponding to reduced *b* hemes, but only a small shoulder around 552 nm corresponding to heme c_1 in the purified complex (Figure 3Bb,d, solid line). This is in contrast to the wild type and M185K, where the contributions from heme c_1 are conspicuous (Figure 3Ba,c, solid line). These simple tests indicate that heme c_1 of M185K is relatively high in redox potential compared to those of the other mutants and suggest that M185H may be photosynthetically incompetent because its potential is too low.

Redox Midpoint Potential of Heme c_1 in M185 Mutants. Although ascorbate provides a rough estimate of relative

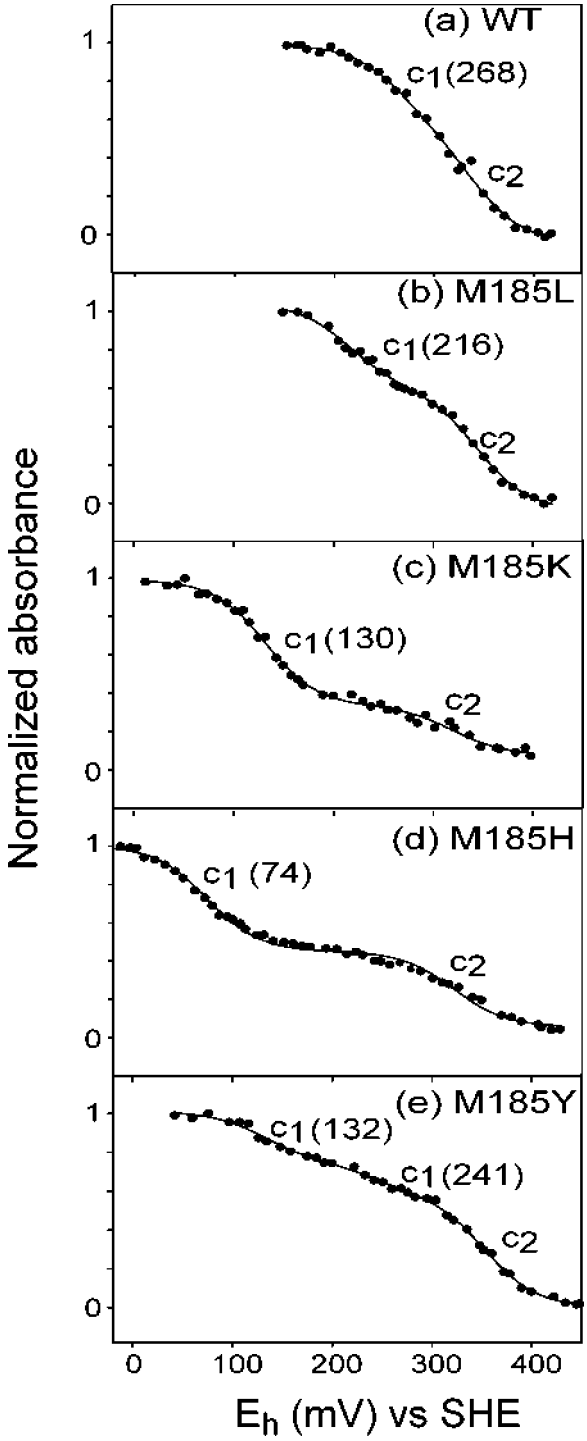

FIGURE 4: Redox titration of various chromatochrome membranes: (a) BC17C (wild type) monitored at 551−570 nm, (b) the M185L mutant monitored at 550−570 nm, (c) the M185K mutant monitored at 550−570 nm, (d) the M185H mutant monitored at 551−570 nm, and (e) the M185Y mutant monitored at 550−570 nm.

redox potentials, the ascorbate/dehydroascorbic acid redox couple suffers from an often irreversible degradation of the dehydroascorbic acid and the interference of oxygen (*31*); this prevents an accurate setting of the redox poise and a dependable measure of the redox midpoint potentials. These problems are prevented by performing conventional equilibrium redox titrations under anaerobic conditions with redox mediator dyes. Redox titrations of the cytochrome α-band region of chromatophores (Figure 4) include contributions from heme c_1 and other high-potential cytochromes (predominantly cytochrome c_2 with an E_m value of 350 mV (*32*)). The second component with a lower E_m value, clearly separable from cytochrome c_2 in all mutants, is assigned to cytochrome c_1. The wild-type E_m of cytochrome c_1 is 268 mV in chromatophores. A similar E_m is seen in the cytochrome c_2-free preparations of purified cytochrome bc_1 (data not shown). In the sixth ligand mutants, the E_m is lowered by approximately 50, 140, and 200 mV (M185L, M185K, and M185H, respectively). Unexpectedly, M185L exhibits a higher redox midpoint potential than M185K, even though M185L is more difficult to reduce with ascorbate. We consider this discrepancy an example of the difficulty of accurately establishing redox potentials in the simple and popular aerobic ascorbate addition assay. The 200 mV drop in M185H is apparently large enough to result in the loss of function reflected in the Ps− phenotype, while the smaller drops of the other mutants apparently allow sufficient electron throughput for maintenance of the Ps+ phenotype.

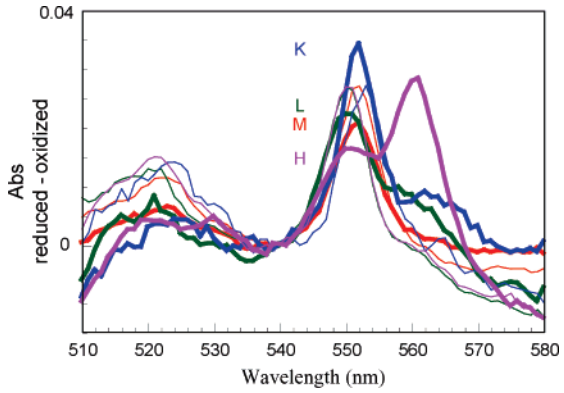

FIGURE 5: Comparison of the cytochrome c_2 (thin lines) and cytochrome c_1 (thick lines) redox difference spectra in chromatophores of wild-type (M) and mutants M185K, -L, and -H. Cytochrome c_2-dominated spectra reflect the first half of the reductive titrations shown in Figure 4 and cytochrome c_1-dominated spectra the second half. Amplitudes of the titrations were normalized according the cytochrome c_2 α-band intensity. Cytochrome c_1 spectra include a progressively greater contribution from heme b_H reduction at 560 nm as the redox midpoint potential of cytochrome c_1 approaches that of b_H in the mutants. There is no obvious low-spin to high-spin transition of cytochrome c_1 in these spectra.

Large drops in potentials in cytochromes are typically associated with significant alterations in the structure and integrity of the heme-binding pocket, which in turn might render the heme more prone to binding by an exogenous ligand such as carbon monoxide (CO), azide, or cyanide. Figure 6 shows dithionite-reduced spectra of purified cytochrome bc_1 before and after exposure to CO in the wild type and selected mutants. The disappearance of the 552 nm peak upon CO binding is clearly seen only in the M185H mutant (Figure 6b). M185K, M185L, and the wild type do not bind CO (Table 1). Thus, the largest drop in redox potential is correlated with CO binding. It appears that *Rb. sphaeroides* maintains more robust heme pocket integrity or heme sixth ligand binding after mutation than the related *Rb. capsulatus*, where all three corresponding mutants, M183L, M183K, and M183H, exhibit heme c_1 redox potentials comparable to or lower than that of M185H in *Rb. sphaeroides*, along with ready binding of CO and loss of photosynthetic competence (Figure 6d and refs *16* and *20*). If photosynthetic incompetence is associated with lower redox potentials, this should

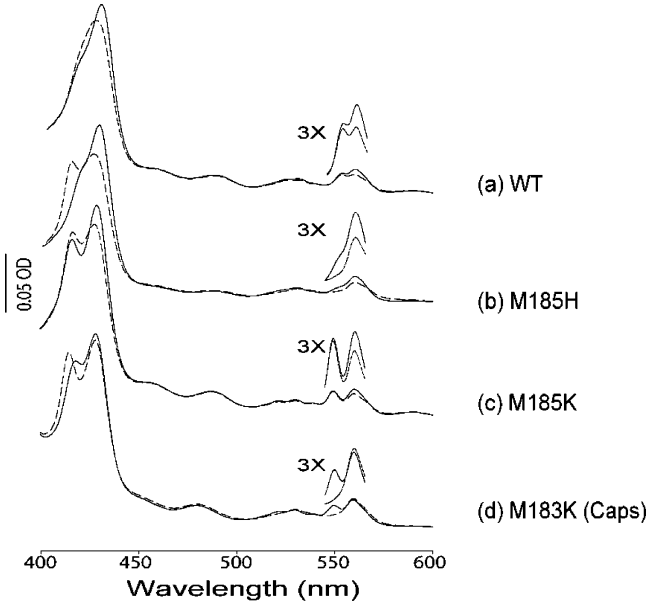

FIGURE 6: CO optical spectra of 2 μM cytochrome bc_1 isolated from the wild type (a), M185H (b), and M185K (c) from *Rb. sphaeroides* and M183K (d) from *Rb. capsulatus*. Insets show enlarged spectra in the α-band region. The solid lines are the dithionite-reduced spectra, and the dashed lines are the dithionite-reduced + CO spectra.

be visible in flash-induced electron transfer kinetics.

When the redox titrations of chromatophore preparations shown in Figure 4 are divided into high- and low-potential halves to separate the spectral signatures dominated by cytochrome c_2 and c_1, respectively (Figure 5), the conspicuous α- and β-bands associated with low-spin heme remain for all the mutants, with no obvious band shift or shape change that is typically associated with loss of a sixth strong field ligand and conversion to a high-spin heme form (*5*). This is true even for M185H which binds CO and may be expected to have weakened sixth ligand binding. The cytochrome c_1 to c_2 α-band peak ratio is smaller for this mutant, which leaves open the possibility that a minor population of low-spin heme with a broader absorption band may be present. On the other hand, M185H may instead have a smaller extinction coefficient or the cytochrome c_2:cytochrome bc_1 ratios may differ slightly in the different strains. The absence of visible spectral evidence of high-spin character was also reported in comparable CO binding mutants in *Rb. capsulatus* (*16*, *20*).

Kinetic Properties of M185 Mutants. If chromatophores are redox poised with the quinone pool reduced, electron transfer in cytochrome bc_1 can be initiated by flash activation of the photosynthetic reaction center to oxidize cytochrome c_2 and deliver oxidants to the high-potential chain of heme c_1 and FeS. Figure 7 shows the time course of flash-induced oxidation of reduced QH_2 at the Q_o site with reduction of heme b_H. In the presence of antimycin, which eliminates the Q_i site activity and reveals the full extent of reduced heme b_H, the reduction of heme b_H takes place on a millisecond time scale in the wild type, M185L, and M185K, but not in M185H. The 10- and 40-fold deceleration of heme *b* reduction in M185L and M185K relative to that in the wild type (Table 1) correlates with the increasing drop in heme c_1 midpoint potential. The absence of b_H heme reduction on this time scale in M185H indicates that a 200 mV E_m drop imposes such a large thermodynamic barrier that physiological electron relay function is lost.

Spontaneous Reversion of the M185H Mutant to the Ps+ Phenotype. When incubated under photosynthetic conditions, the Ps− strain carrying the M185H mutation spontaneously reverts to Ps+. DNA sequence analysis of several of the revertant strains reveals that H is replaced with either L, a Ps+ strain we have already described, or Y (Table 1). Further characterization shows that M185Y assembles all four subunits with the heme group covalently attached to cytochrome c_1 (Figure 2). The difference absorption spectra reveal that M185Y reversion raises the midpoint potential of cytochrome c_1 so it becomes partially reducible by ascorbate (Figure 3Ae,3Be). Redox titration shows that the heme c_1 in M185Y has moved back up to the redox range displayed by other Ps+ mutants, M185K and M185L, although the redox behavior is heterogeneous, splitting into two components of 132 and 241 mV (Figure 4e and Table 1). The inability of M185Y to bind CO shows that the revertant restores the integrity of the heme-binding pocket and axial ligation (Table 1). The increase in E_m also restores electron transfer activity (Figure 7e) with flash-induced reduction of heme b_H at a rate comparable to those seen in other Ps+ mutants (Table 1).

DISCUSSION

Of the physical factors associated with determining the redox midpoint potential of *c* hemes in proteins, the nature of the sixth ligand is primarily important. The electron withdrawing ability of the sulfur of Met as a ligand to the Fe tends to stabilize the reduced form and hence increase the E_m. The electron donating ability of the N of His tends to stabilize the oxidized form and lower the E_m (*1*, *4*, *33*). Thus, from sixth ligand concerns alone, we expect that removing the Met should allow the E_m to drop and that introducing a His will actively lower the E_m. This pattern describes what is seen in *Rb. capsulatus* (*16*, *20*).

However, the pattern of redox midpoint modulation in sixth ligand mutants in *Rb. sphaeroides* is conspicuously different from that of *Rb. capsulatus*. Except for the His mutants, the E_m did not drop down to the low and photosynthetically incompetent level characteristic of all sixth ligand mutants in *Rb. capsulatus*. This suggests that there are other factors operating in *Rb. sphaeroides* that support the high redox potential.

The second physical factor classically associated with modulation of the E_m of *c* hemes is solvent accessibility: restricting the approach of water to the heme helps maintain a relatively low polarity of the heme environment which destabilizes the highly charged oxidized heme and thus raises the E_m (*34*). Another factor related to polarity is the relatively tight packing or "contraction" of the residues around the heme, perhaps through a hydrogen-bond network, which similarly tends to increase the E_m (*4*, *33*, *35*). L, K, and H substitutions for M in *Rb. capsulatus* all seem to open or loosen the heme pocket, as witnessed by CO accessibility and binding, and all show a conspicuous drop in E_m to nonfunctional values. In *Rb. sphaeroides*, only the H substitution seems to have sufficiently disrupted the organization of the pocket to allow CO binding. It appears that *Rb. sphaeroides* has some additional heme pocket integrity

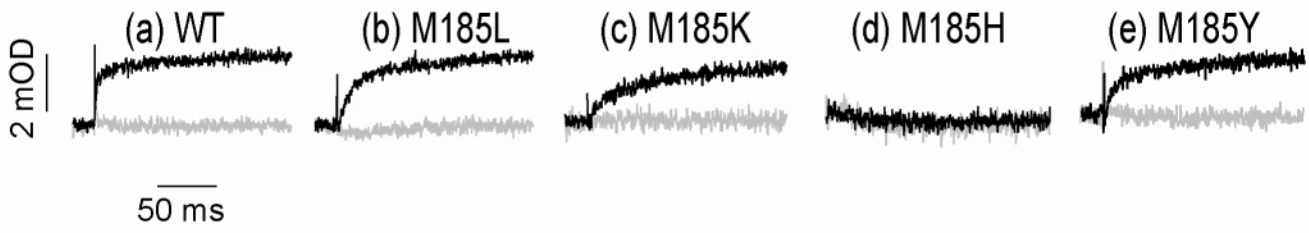

FIGURE 7: Flash kinetics of heme b_H reduction in chromatophores from the wild type (a), M185L (b), M185K (c), M185H (d), and M185Y (e). The ambient redox potential was poised at 100 mV and pH 7.0. The kinetics of the flash-induced reduction of heme b_H were followed at 560−570 nm. Q_i site reaction is inhibited with antimycin (black); in the control, both Q_i and Q_o site activity is inhibited with antimycin and myxothiazol (gray).

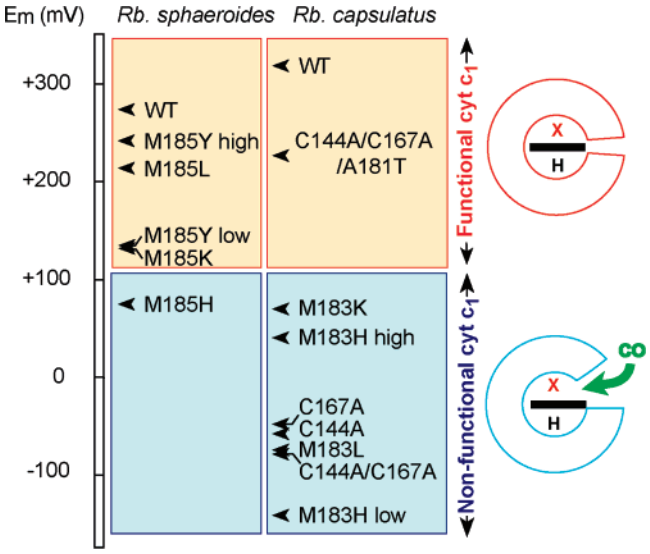

FIGURE 8: Schematic illustration of structural integrity and redox potential changes of cytochrome (cyt) c_1 in *Rb. sphaeroides* and *Rb. capsulatus* (*10*, *16*, *20*). Cytochrome c_1 midpoint potentials fall into two categories, photosynthetically functional (red) and non-functional (blue) which are associated with potentials above and below an ~100 mV threshold and a "closed" and "open" heme environment that forbids or allows CO binding.

maintaining motifs not present in *Rb. capsulatus*. A schematic view of this model is shown in Figure 8, which also summarizes the midpoint changes of the various mutants in the two species.

The wild-type form of *Rb. sphaeroides* cytochrome bc_1 has two identifiable motifs that have been associated with E_m increasing solvent inaccessibility and packing: a disulfide-secured loop immediately preceding the sixth axial ligand position (also present in *Rb. capsulatus*) and a βXM motif. The latter motif with a β-branched amino acid two residues before the sixth ligand position is associated with the high-potential *c* hemes of cytochrome c_8 and mitochondrial cytochrome *c* (*5*, *36*). The β-branch motif is not present in wild-type *Rb. capsulatus* but was spontaneously introduced as a revertant from a low-potential, photosynthetically incompetent mutant in which the disulfide bond was removed (*10*). It seems possible that the β-branched amino acid motif may promote a more secure packing in the heme pocket and help maintain a higher E_m in *Rb. sphaeroides* even when the liganding M is replaced. Wild-type *Rb. capsulatus* achieves a higher E_m than *Rb. sphaeroides* but cannot avoid collapsing to low potential when the Met is lost, a fate the apparently more resilient *Rb. sphaeroides* heme packing avoids.

The importance of the disulfide-secured loop in supporting high heme c_1 redox potentials has been established in *Rb. capsulatus* (*10*). Breaking the disulfide reduces the E_m to incompetent levels which can be repaired, for example, by the βXM revertant just discussed. However, *Rb. sphaeroides* once again appears to be more resilient than *Rb. capsulatus* in maintaining a high, physiologically competent E_m in heme c_1. Not only can the disulfide be mutationally broken (*37*), but a double mutant that both breaks the disulfide and removes the βXM motif is also physiologically competent (H. Zhang et al., manuscript in preparation). Thus the redox resilience of *Rb. sphaeroides* must include other elements beyond these disulfide and βXM motifs.

At this point, we cannot be certain about the identity of the heme ligands in the *Rb. sphaeroides* mutants. We do know that the analogous M183K and M183H mutants in *Rb. capsulatus* were shown by MCD and EPR to be mostly amine- and histidine-ligated, respectively (*38*, *39*). However, in purified complexes, it appeared that there was enough flexibility in the sixth ligand region to accommodate a minor, variable amount of bis-His ligation in both the wild-type and M183K forms (*39*). Indeed, in the *Rb. capsulatus* M183L mutant, in which the leucine can provide neither an amine nor an imidazole ligand to the heme iron, conformational flexibility of this sixth ligand loop is enough to allow a remote histidine to be recruited as the sixth ligand and depress the E_m significantly, at least in purified cytochrome bc_1. This bis-histidyl geometry of *Rb. capsulatus* cytochrome c_1 may be a folding intermediate akin to that seen in mitochondrial cytochrome *c* (*16*, *40*, *41*). The observation here in *Rb. sphaeroides* that the redox midpoint potential does not drop down to characteristic bis-His levels upon removal of the Met ligand is an indication of the relative robustness and generally lower conformational flexibility of the protein loops on the sixth ligand side of *Rb. sphaeroides*. Even the unligatable Leu replacement seems to have little tendency to attract a remote E_m-lowering histidine. The revertant M185Y, which increases the E_m from the nonfunctional M185H level to a photosynthetically competent level, may have slightly more conformational flexibility in the heme pocket, as the only example of a sixth ligand mutant in this species that displays the heterogeneity of two redox potentials for heme c_1. However, even this revertant is apparently not so open and flexible to allow CO to bind and is included in the upper "closed" heme pocket category of Figure 8 along with all other sixth ligand mutants of *Rb. sphaeroides* except M185H.

Although *Rb. sphaeroides* has used multiple motifs to ensure a high redox midpoint potential for heme c_1, when

the E_m drops below the threshold somewhere between 140 and 200 mV below that of the wild type, the photosynthetic competence is seriously compromised. Presumably, this reflects the tendency of relatively low-potential heme c_1 to sequester oxidizing equivalents in the high-potential chain and to make it more difficult for the higher-potential FeS cluster to offer an oxidant to the Q_o site for quinone oxidation and energy transduction when oxidizing equivalents are limiting. At pH 7 in the wild type, heme c_1 is already almost 50 mV below the E_m of FeS and is 6 times more likely to be oxidized than FeS under oxidant-limited conditions. However, this redox difference still allows the FeS to be sufficiently oxidized transiently so that the rate of Q_o site turnover is not limited by FeS oxidation. The rate of Q_o site oxidation begins to become conspicuously slow when heme c_1 falls ~100 mV below the FeS midpoint in the M185L mutant, and heme c_1 is ~50 times more likely to hold the oxidant compared to FeS. A detailed modeling of the electron tunneling network in response to mutant driving force changes will be provided in another report. Even the approximately 180 mV difference in FeS and heme c_1 E_m values in M185K which favors c_1 oxidation by 3 orders of magnitude can still muster enough electron transfer through cytochrome bc_1 to support photosynthetic growth. This is near the limit, however, because pushing the redox equilibrium between FeS and heme c_1 to the next order of magnitude results in failure. It appears that the robust design of redox components in the high-potential chain of cytochrome bc_1 places them close enough so that rapid (normally microsecond) electron tunneling can distribute oxidizing and reducing equivalents as required for electron transfer relay and catalytic function under a remarkably wide range of conditions but that a 3−4 order of magnitude unfavorable redox equilibrium represents the limit of accommodation for this design.

ACKNOWLEDGMENT

We thank C. A. Wraight (Department of Biochemistry, University of Illinois, Urbana, IL) for providing us with the cytochrome bc_1 expression system for *Rb. sphaeroides*.

REFERENCES

1. Battistuzzi, G., Borsari, M., and Sola, M. (2001) Medium and Temperature Effects on the Redox Chemistry of Cytochrome c, *Eur. J. Inorg. Chem.*, 2989−3004.
2. Battistuzzi, G., Borsari, M., and Sola, M. (2001) Redox properties of cytochrome c, *Antioxid. Redox Signaling 3*, 279−91.
3. Meyer, T. (1996) *Evolution and classification of c-type cytochromes*, University Science Books, Sausalito, CA.
4. Dolla, A., Blanchard, L., Guerlesquin, F., and Bruschi, M. (1994) The protein moiety modulates the redox potential in cytochromes c, *Biochimie 76*, 471−9.
5. Moore, G. R., and Pettigrew, G. W. (1990) *Cytochrome c: Evolutionary, structural and physicochemical aspects*, Springer-Verlag, Berlin.
6. Berry, E., Huang, L.-S., Saechao, L., Pon, N., Valkova-Valchanova, M., and Daldal, F. (2004) X-Ray Structure of *Rhodobacter capsulatus* Cytochrome bc_1: Comparison with its Mitochondrial and Chloroplast Counterparts, *Photosynth. Res. 81*, 251−75.
7. Zhang, Z., Huang, L., Shulmeister, V. M., Chi, Y. I., Kim, K. K., Hung, L. W., Crofts, A. R., Berry, E. A., and Kim, S. H. (1998) Electron transfer by domain movement in cytochrome bc_1, *Nature 392*, 677−84.
8. Iwata, S., Lee, J. W., Okada, K., Lee, J. K., Iwata, M., Rasmussen, B., Link, T. A., Ramaswamy, S., and Jap, B. K. (1998) Complete structure of the 11-subunit bovine mitochondrial cytochrome bc_1 complex, *Science 281*, 64−71.
9. Xia, D., Yu, C. A., Kim, H., Xia, J. Z., Kachurin, A. M., Zhang, L., Yu, L., and Deisenhofer, J. (1997) Crystal structure of the cytochrome bc_1 complex from bovine heart mitochondria, *Science 277*, 60−6.
10. Osyczka, A., Dutton, P. L., Moser, C. C., Darrouzet, E., and Daldal, F. (2001) Controlling the functionality of cytochrome c_1 redox potentials in the *Rhodobacter capsulatus* bc_1 complex through disulfide anchoring of a loop and a β-branched amino acid near the heme-ligating methionine, *Biochemistry 40*, 14547−56.
11. Yun, C. H., Beci, R., Crofts, A. R., Kaplan, S., and Gennis, R. B. (1990) Cloning and DNA sequencing of the fbc operon encoding the cytochrome bc_1 complex from *Rhodobacter sphaeroides*. Characterization of fbc deletion mutants and complementation by a site-specific mutational variant, *Eur. J. Biochem. 194*, 399−411.
12. Yu, L., Dong, J. H., and Yu, C. A. (1986) Characterization of purified cytochrome c_1 from *Rhodobacter sphaeroides* R-26, *Biochim. Biophys. Acta 852*, 203−11.
13. Konishi, K., Van Doren, S. R., Kramer, D. M., Crofts, A. R., and Gennis, R. B. (1991) Preparation and characterization of the water-soluble heme-binding domain of cytochrome c1 from the *Rhodobacter sphaeroides* bc_1 complex, *J. Biol. Chem. 266*, 14270−6.
14. Furbacher, P. N., Tae, G.-S., and Cramer, W. A. (1996) *Evolution and origins of the cytochrome bc_1 and b_6f complex*, VCH, New York.
15. Miller, G. T., Zhang, B., Hardman, J. K., and Timkovich, R. (2000) Converting a c-type to a b-type cytochrome: Met61 to His61 mutant of *Pseudomonas* cytochrome c-551, *Biochemistry 39*, 9010−7.
16. Darrouzet, E., Mandaci, S., Li, J., Qin, H., Knaff, D. B., and Daldal, F. (1999) Substitution of the sixth axial ligand of *Rhodobacter capsulatus* cytochrome c_1 heme yields novel cytochrome c_1 variants with unusual properties, *Biochemistry 38*, 7908−17.
17. Lo, T. P., Komar-Panicucci, S., Sherman, F., McLendon, G., and Brayer, G. D. (1995) Structural and functional effects of multiple mutations at distal sites in cytochrome c, *Biochemistry 34*, 5259−68.
18. Lu, Y., Casimiro, D. R., Bren, K. L., Richards, J. H., and Gray, H. B. (1993) Structurally engineered cytochromes with unusual ligand-binding properties: Expression of *Saccharomyces cerevisiae* Met-80 → Ala iso-1-cytochrome c, *Proc. Natl. Acad. Sci. U.S.A. 90*, 11456−9.
19. Wallace, C. J., and Clark-Lewis, I. (1992) Functional role of heme ligation in cytochrome c. Effects of replacement of methionine 80 with natural and non-natural residues by semisynthesis, *J. Biol. Chem. 267*, 3852−61.
20. Gray, K. A., Davidson, E., and Daldal, F. (1992) Mutagenesis of methionine-183 drastically affects the physicochemical properties of cytochrome c_1 of the bc_1 complex of *Rhodobacter capsulatus*, *Biochemistry 31*, 11864−73.
21. Raphael, A. L., and Gray, H. B. (1991) Semisynthesis of axial-ligand (position 80) mutants of cytochrome, *J. Am. Chem. Soc. 113*, 1038−40.
22. Nakai, M., Ishiwatari, H., Asada, A., Bogaki, M., Kawai, K., Tanaka, Y., and Matsubara, H. (1990) Replacement of putative axial ligands of heme iron in yeast cytochrome c_1 by site-directed mutagenesis, *J. Biochem. 108*, 798−803.
23. Raphael, A. L., and Gray, H. B. (1989) Axial ligand replacement in horse heart cytochrome c by semisynthesis, *Proteins 6*, 338−40.
24. Keen, N. T., Tamaki, S., Kobayashi, D., and Trollinger, D. (1988) Improved broad-host-range plasmids for DNA cloning in Gram-negative bacteria, *Gene 70*, 191−7.
25. Valkova-Valchanova, M. B., Saribas, A. S., Gibney, B. R., Dutton, P. L., and Daldal, F. (1998) Isolation and characterization of a two-subunit cytochrome b-c_1 subcomplex from *Rhodobacter capsulatus* and reconstitution of its ubihydroquinone oxidation (Q_o) site with purified Fe-S protein subunit, *Biochemistry 37*, 16242−51.
26. Atta-Asafo-Adjei, E., and Daldal, F. (1991) Size of the amino acid side chain at position 158 of cytochrome b is critical for an active cytochrome bc_1 complex and for photosynthetic growth of *Rhodobacter capsulatus*, *Proc. Natl. Acad. Sci. U.S.A. 88*, 492−6.
27. Laemmli, U. K. (1970) Cleavage of structural proteins during the assembly of the head of bacteriophage T4, *Nature 227*, 680−5.

28. Thomas, P. E., Ryan, D., and Levin, W. (1976) An improved staining procedure for the detection of the peroxidase activity of cytochrome P-450 on sodium dodecyl sulfate polyacrylamide gels, *Anal. Biochem. 75*, 168−76.
29. Dutton, P. L. (1978) Redox potentiometry: Determination of midpoint potentials of oxidation-reduction components of biological electron-transfer systems, *Methods Enzymol. 54*, 411−35.
30. Osyczka, A., Moser, C. C., Daldal, F., and Dutton, P. L. (2004) Reversible redox energy coupling in electron transfer chains, *Nature 427*, 607−12.
31. Clark, W. M. (1960) *Oxidation-reduction potentials of organic systems*, Willams & Wilkins, Baltimore.
32. Pettigrew, G. W., Meyer, T. E., Bartsch, R. G., and Kamen, M. D. (1976) pH dependence of the oxidation-reduction potential of cytochrome c_2, *Biochim. Biophys. Acta 430*, 197−208.
33. Caffrey, M. S., Daldal, F., Holden, H. M., and Cusanovich, M. A. (1991) Importance of a conserved hydrogen-bonding network in cytochromes c to their redox potentials and stabilities, *Biochemistry 30*, 4119−25.
34. Kassner, R. J. (1972) Effects of nonpolar environments on the redox potentials of heme complexes, *Proc. Natl. Acad. Sci. U.S.A. 69*, 2263−7.
35. Gunner, M. R., and Honig, B. (1991) Electrostatic control of midpoint potentials in the cytochrome subunit of the *Rhodopseudomonas viridis* reaction center, *Proc. Natl. Acad. Sci. U.S.A. 88*, 9151−5.
36. Ambler, R. P. (1996) The distance between bacterial species in sequence space, *J. Mol. Evol. 42*, 617−30.
37. Elberry, M., Yu, L., and Yu, C. A. (2006) The disulfide bridge in the head domain of *Rhodobacter sphaeroides* cytochrome c_1 is needed to maintain its structural integrity, *Biochemistry 45*, 4991−7.
38. Li, J., Darrouzet, E., Dhawan, I. K., Johnson, M. K., Osyczka, A., Daldal, F., and Knaff, D. B. (2002) Spectroscopic and oxidation-reduction properties of *Rhodobacter capsulatus* cytochrome c_1 and its M183K and M183H variants, *Biochim. Biophys. Acta 1556*, 175−86.
39. Finnegan, M. G., Knaff, D. B., Qin, H., Gray, K. A., Daldal, F., Yu, L., Yu, C. A., Kleis-San Francisco, S., and Johnson, M. K. (1996) Axial heme ligation in the cytochrome bc_1 complexes of mitochondrial and photosynthetic membranes. A near-infrared magnetic circular dichroism and electron paramagnetic resonance study, *Biochim. Biophys. Acta 1274*, 9−20.
40. Yeh, S. R., and Rousseau, D. L. (1998) Folding intermediates in cytochrome c, *Nat. Struct. Biol. 5*, 222−8.
41. Xu, Y., Mayne, L., and Englander, S. W. (1998) Evidence for an unfolding and refolding pathway in cytochrome c, *Nat. Struct. Biol. 5*, 774−8.
42. Hunte, C., Koepke, J., Lange, C., Rossmanith, T., and Michel, H. (2000) Structure at 2.3 Å resolution of the cytochrome bc_1 complex from the yeast *Saccharomyces cerevisiae* co-crystallized with an antibody Fv fragment, *Structure 8*, 669−84.

BI061345I